

## EFFECT OF QUASI-ORTHOGONAL EMISSION MODES ON THE ROTATION MEASURES OF PULSARS

R. RAMACHANDRAN AND D. C. BACKER

Department of Astronomy, University of California, Berkeley, CA 94720-3411; ramach@astro.berkeley.edu, dbacker@astro.berkeley.edu

JOANNA M. RANKIN

Physics Department, University of Vermont, Burlington, VT 05405; joanna.rankin@uvm.edu

AND

J. M. WEISBERG AND K. E. DEVINE

Department of Physics and Astronomy, Carleton College, Northfield, MN 55057; jweisber@carleton.edu

Received 2003 September 16; accepted 2004 January 26

### ABSTRACT

We report here the discovery of a significant source of systematic error in the determinations of pulsar rotation measures. Conventional analysis of high-sensitivity polarimetric observations of PSR B2016+28 display variation in the rotation measure of  $\pm 15 \text{ rad m}^{-2}$  (around the mean value of  $-34.6 \text{ rad m}^{-2}$ ) across the pulse profile. Analysis of single pulse data shows that this variation is an artifact of the incoherent superposition of quasi-orthogonal polarization modes along with the frequency dependence of relative strength and/or quasi-orthogonality of the modes. Quasi-orthogonal polarization is common among pulsars, and therefore this effect needs to be taken into account in the interpretation of pulsar rotation measures.

*Subject headings:* ISM: magnetic fields — polarization — pulsars: individual (PSR B2016+28) — radiation mechanisms: nonthermal — radio continuum: stars

### 1. INTRODUCTION

Pulsars play a major role in our understanding of interstellar magnetic field structure through measurements as a function of radio frequency of Faraday rotation of the plane of linear polarization introduced by the component of the field along the sight line in the warm interstellar medium ( $B_{\parallel}$ ). The standard definition of rotation measure (RM) in cgs. units is given by

$$\text{RM} = \frac{e^3}{2\pi m_e^2 c^4} \int_0^L n_e(l) B_{\parallel}(l) dl \quad (1)$$

where  $L$  is the distance to the pulsar from the observer,  $dl$  is the length element along the line of sight,  $n_e$  is the free electron number density,  $e$  and  $m_e$  are the charge and the mass of an electron, and  $c$  is the velocity of light in vacuum. The amount of rotation experienced by the intrinsic linear polarization position angle of the source ( $\psi_0$ ) at a given wavelength ( $\lambda$ ) is expressed as

$$\psi - \psi_0 = \text{RM} \lambda^2, \quad (2)$$

where  $\psi$  is the apparent linear polarization position angle (P.A.) as seen by the observer. Several investigators have measured RM values of pulsars (Manchester 1972, 1974; Hamilton & Lyne 1987; Rand & Lyne 1994; Guojun et al. 1995; Weisberg et al. 2004). Time dependence in the measured RM values<sup>1</sup> has also been noted for some pulsars, like those in the Vela and Crab supernova remnants (Hamilton et al. 1977; Rankin et al. 1988). A positive RM means the magnetic field direction is toward the observer, and a negative RM means the direction is away. Using the measured values, detailed modelling of magnetic field structure has been

carried out by several authors (Thompson & Nelson 1980; Indrani & Deshpande 1998; Han, Manchester, & Qiao 1999, 2002; Mitra et al. 2003). All of these galactic models based on pulsar RMs have as central assumptions that the RM is completely determined by the interstellar medium and that the magnetosphere of the pulsar, with all of its complexities, does not contribute significantly.

We show in this paper that a conventional RM analysis based on average pulse profiles leads to large variations of the RM across the pulse profile of PSR B2016+28. The conventional analysis requires some form of averaging to arrive at a single RM. Additional work that we are doing has shown that this effect occurs in other pulsars as well. In pulsars with significant RM variations across the pulse profile, this is a source of error that may not have been considered in past modeling of galactic magnetic fields.

Significant magneto-ionic propagation effects are not expected in pulsar magnetospheres because of the ultra-relativistic nature of the plasma. Any large Faraday rotation within the emission region of the magnetosphere would lead to severe depolarization across our band. The fact that pulsar radiation is highly polarized therefore shows that there is no significant Faraday rotation within the emission region. We are led then to look more closely at the data to determine the nature of the RM variations across the pulse.

We show an improved method for RM determination when sufficient signal-to-noise ratio (S/N) allows detection of the pulsed radiation in single pulses. In this case, the orthogonal modes of polarization (e.g., Backer & Rankin 1980) can be identified, and the RM can be determined from each mode independently. If the modes were strictly orthogonal *and* there was no jitter *and* there was no frequency dependence of these properties, then this procedure would not be necessary. However, the P.A.s (position angles) at each longitude do display jitter and a slight degree of nonorthogonality (Gil, Snakowski & Stinebring 1991; Gil et al. 1992). We show that the B2016+28 emission has a slight frequency dependence in

<sup>1</sup> It is also important to compensate for the variable ionospheric contribution to the measured RM values. As Manchester (1972) states, this contribution could be as high as 0.1 to 6  $\text{rad m}^{-2}$ , depending on the time of the day and the declination of the pulsar.

TABLE 1  
DEFINITION OF VARIABLES

Variable	Definition
$\phi$ .....	Pulse longitude
P.A. ....	Linear polarization position angle
RM .....	Rotation measure
$RM(\phi)$ .....	Rotation measure at a given longitude $\phi$ measured with average pulse profiles
$RM_A(\phi)$ .....	Rotation measure of polarization mode A
$RM_B(\phi)$ .....	Rotation measure of polarization mode B
S/N .....	Signal-to-noise ratio
$\chi_A(\phi, \nu), \chi_B(\phi, \nu)$ .....	Weighted mean values of linear polarization position angles of modes A and B
$\langle \chi_{AB}(\nu) \rangle$ .....	Linear polarization position angle at a given frequency after incoherently superposing the two (non)orthogonal modes
$X_A(t, \nu), X_B(t, \nu)$ .....	Linear polarization intensities of the two modes as a function of time and frequency
$X_N(t, \nu)$ .....	System noise power as a function of time and frequency
$\langle RM \rangle$ .....	Net RM value computed from average pulse profile after averaging over all pulse longitudes.

the relative strengths and (or) amounts of nonorthogonality. This is the source of the pulse-longitude dependence of the RM in the conventional analysis. One does not have to appeal to strong, and unexpected, magneto-ionic propagation effects.

Most pulsars for which single pulses have been studied show signs of orthogonal modes in their emission. The problem of origin of these modes has been addressed by several investigators (e.g., Melrose 1979; Petrova & Lyubarskii 2000; Radhakrishnan & Deshpande 2001; Petrova 2001). As they describe, the orthogonal mode could arise from the partial conversion of an original mode (ordinary) to the other (extraordinary) during propagation in the magnetosphere of the pulsar. Even the cause for the slight nonorthogonality has been addressed by investigators like Petrova (2001).

In this paper, after briefly describing the details of our observations in § 2, we summarize the conventional approach to RM determination in § 3. Here we describe the aforementioned RM variations as a function of pulse longitude for PSR B2016+28. In §§ 4 and 5 we show how quasi-orthogonal modes in pulsars can cause severe artifacts in RM estimations, and in particular how the apparent variations in the RM of PSR B2016+28 can be produced. We conclude our analysis with a detailed discussion in § 6. The symbols for variables used in this paper are defined in Table 1.

## 2. OBSERVATIONS

The average pulse observations were performed at the Arecibo Observatory at 430 MHz in 1992 May and December with a bandwidth of 5 MHz. Average pulse profiles were produced by integrating the signal in each frequency channel for 120 s. The observation setup is described in detail in Weisberg et al. (2004).

The single-pulse observations were carried out at Arecibo Observatory at 430 MHz center frequency in a single session in 1992 October. With a special program for gating the 40 MHz correlator, auto-correlation and cross-correlation functions of the right-hand and left-hand polarization channel voltages were recorded with 32 correlation lags. The bandwidth of the observation was 10 MHz. The correlation vectors were averaged to a time resolution of 506  $\mu$ s. The correlation data were three-level corrected after scaling and Fourier transformed to produce Stokes parameter spectra. A detailed calibration procedure was adopted to correct for instrumental effects, delays, and interstellar dispersion. These observations, as well as calibration procedures, have been described in Rankin & Rathnasree (1995). The resulting polarized pulse sequence had 32 channels

(although channel 1 lacked Stokes  $U$  and thus was unusable) with 3043 pulses (1600 s) and was gated to include a longitude range of  $\sim 45^\circ$ . A constant RM value of  $-34.6 \text{ rad m}^{-2}$  (an earlier measurement in the literature) was also subtracted from the data.

## 3. CONVENTIONAL RM MEASUREMENTS

As individual pulses from pulsars are usually faint, one typically generates an “average” pulse profile by folding the time series in each frequency channel and Stokes parameter synchronously with the Doppler-shifted apparent period. An important property of radio emission from pulsars is that the position angle of linear polarization changes as a function of pulse longitude (Radhakrishnan & Cooke 1969). Because of this property, RM measurements of pulsars have always been more complex than those for any other polarized radio source in the sky. P.A. measurements using a given longitude bin of folded profiles and all frequency channels are used to fit for the rotation measure [ $RM(\phi)$ ] on the basis of equation 2. This is repeated for each longitude bin, and the RM from all these bins are averaged to estimate the overall value,  $\langle RM \rangle$ , for the pulsar. Of course, the underlying assumption here is that the values measured in all the longitude bins are entirely introduced by only the interstellar medium, and hence there is no longitude-dependent rotation measure introduced by the pulsar itself. Errors in  $RM(\phi)$  can be simply propagated using the S/N of each individual estimate and an assumption of independence of the estimates.

In our analysis, as the first step, we have attempted to compute  $RM(\phi)$  values as a function of pulse longitude. As mentioned above, this has been estimated from the average profiles constructed in each of the 31 frequency channels in our sequence. Figures 1 and 2 summarize the results. Figure 1 shows the results from four different scans from our observations, each of 120 s integration. In the top panel, we give the average pulse profile in Stokes  $I$  parameter (*solid line*), average linearly polarized power (*dashed line*), and average circularly polarized power (*dot-dashed line*). The middle panel shows linear polarization position angle, and the bottom panel shows  $RM(\phi)$ .

In the top panel of Figure 2, the solid line gives the average pulse profile in total power, and the thin dashed line gives the average profile in linear polarization computed from average profiles in all Stokes parameters. This is to be compared with the thick dashed line, which gives linear power computed from single pulses and averaged over all pulses. The thin dashed line shows a smaller degree of linear polarization because of incoherent superposition of the polarization modes.

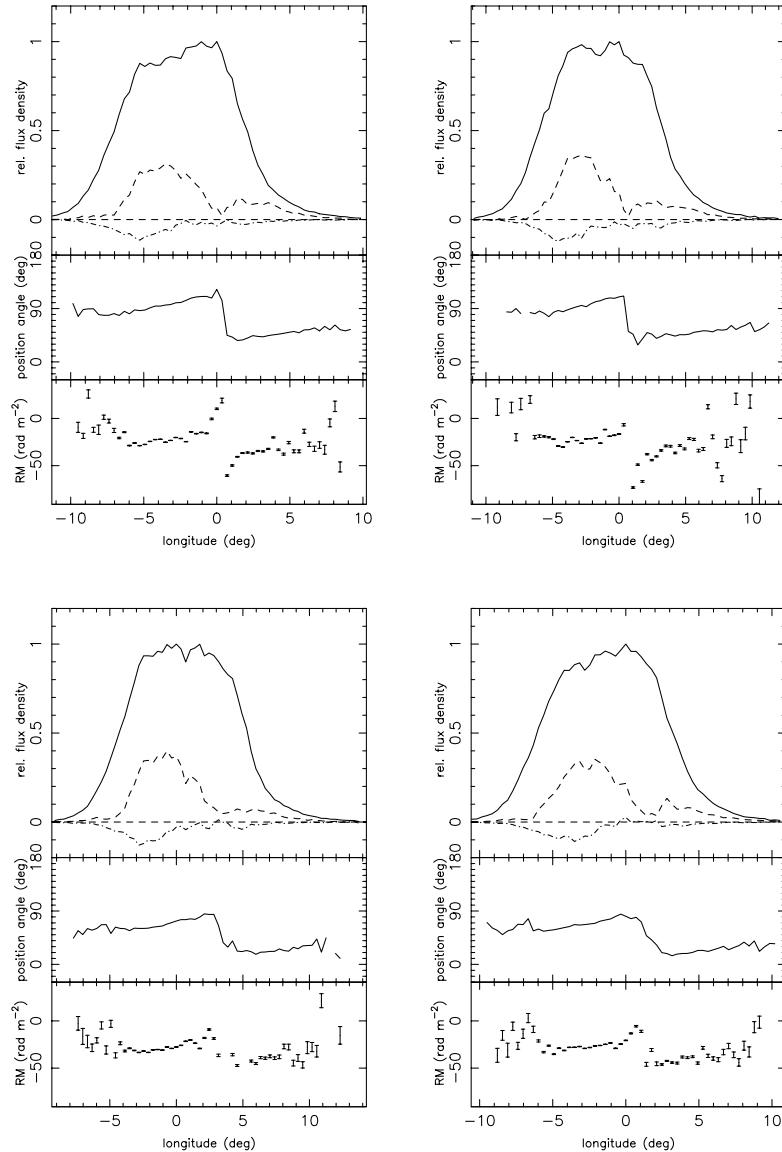


FIG. 1.—Results from four different average-pulse data sets. *Top*: Average profile in Stokes  $I$  parameter (*solid line*), linearly polarized power (*dashed line*) and circularly polarized power (*dot-dashed line*). *Middle*: Linear polarization position angle determined from the average profile. *Bottom*:  $RM(\phi)$  vs.  $\phi$ . See text for details.

The thin dot dashed line indicates power in circular polarization computed from average profiles in the Stokes  $V$  parameter. Negative power indicates left-circular polarization.

The dots in the middle panel give the linear polarization P.A. curve as defined by the average profile, and the gray scale gives the probability density function (PDF) of the position angle computed from all the single pulses. While computing this PDF, we have weighted the values with the square of their S/N ratio of the polarized flux as defined by  $(Q^2 + U^2)^{1/2} / \sigma_{\text{sys}}$  (where  $Q$  and  $U$  are two of the Stokes parameters and  $\sigma_{\text{sys}}$  is the rms value of the system noise flux).<sup>2</sup> Although the P.A. range outside  $\pm 90^\circ$  is redundant, we have chosen a range of  $\pm 180^\circ$  for clarity.

In the bottom panel of Figure 2, we give the measured values of  $RM(\phi)$  as a function of pulse longitude. The dotted line in the bottom panel shows the earlier measurement of

$RM$  for this pulsar (Manchester 1972),  $-34.6 \text{ rad m}^{-2}$ . As we mentioned in § 2, the data that we used for our analysis already had a constant  $RM$  value of  $-34.6 \text{ rad m}^{-2}$  removed from it. But to be consistent, we have added this offset in the plot (*dotted line*). Effective  $RM$  from our measurement comes to  $-38.3 \pm 0.3 \text{ rad m}^{-2}$ , which is significantly different from the earlier measurement of Manchester, as well as of Weisberg et al. (2004), which is  $-27.3 \pm 2.1 \text{ rad m}^{-2}$ .

There are two aspects of Figures 1 and 2 that needs to be discussed here. The measured values of  $RM(\phi)$  as a function of pulse longitude display significant systematic variations. If this effect is true, then it has a very fundamental significance, as one does not expect the interstellar medium to distinguish between one pulse longitude and the other. Therefore, this  $RM$  difference must be due to intrinsic propagation effects in the pulsar magnetosphere. In fact, this would become the first ever direct evidence for propagation effects in the pulsar magnetosphere. However, as we show in § 4, this is due to artifacts introduced by superposition of the two more or less orthogonal emission modes seen in this pulsar.

<sup>2</sup> As the telescope gain of Arecibo Telescope is significantly high, variation of system noise with the strength of the pulsar was explicitly taken into account with the help of the calibrated average pulse profile.

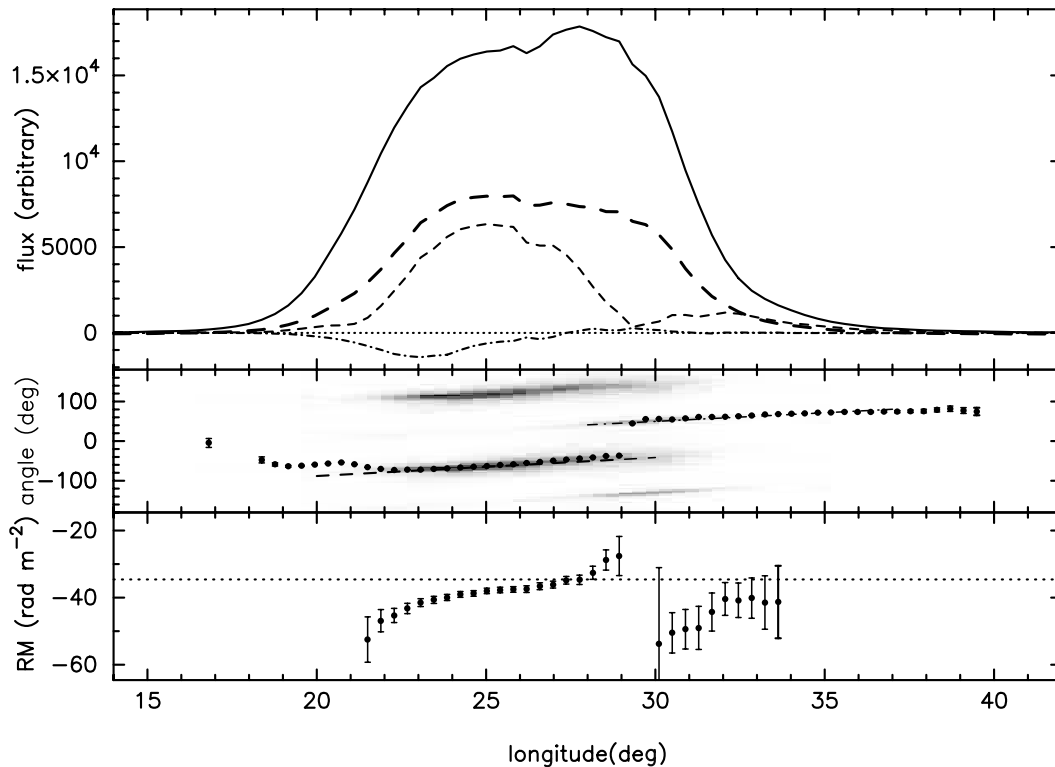


FIG. 2.— $RM(\phi)$  vs.  $\phi$ . *Top*: Average pulse profile in Stokes  $I$  is given as a solid line. Thin and thick dashed lines are linear polarization power computed from average pulses and from single pulses and averaged over all pulses, respectively. The thin dot-dashed line gives circular polarization power (Stokes  $V$ ) computed from average pulses. A horizontal dotted line is drawn to indicate the zero level in the  $y$ -axis. *Middle*: The dots show P.A. estimated from the average profile. The gray scale gives the probability density function of P.A.s estimated from single pulses. *Bottom*:  $RM(\phi)$  estimated from average pulse. The value of  $\langle RM \rangle$  computed from this is  $-38.3 \pm 0.3 \text{ rad m}^{-2}$ .

Secondly, in Figure 1, the overall behavior of  $RM(\phi)$  is similar in all plots. As described in § 2, these data sets were obtained in 1992 May and December. The “antisymmetric” behavior of  $RM(\phi)$  (with respect to longitude value of zero in Fig. 1) seems to be stable over a timescale of several months. However, although the overall behavior of  $RM(\phi)$  is stable, it is quite clear that the exact value of  $RM(\phi)$  is not the same in all the panels of Figure 1. We return to this later in § 6.

RM values varying as a function of pulse longitude are not unique to this pulsar alone. This has already been observed in other pulsars, such as PSR B0329+54 (D. Mitra, S. Johnston, & M. Kramer, 2004, private communication).

#### 4. INTRINSIC $RM(\Phi)$ VARIATIONS?

If the two polarization modes are strictly orthogonal, then they have no effect on conventional RM measurements. When we compute the average profile in each frequency channel, all that we are doing is “incoherently” superposing the radiation from the two orthogonal modes. This would mean that the net degree of polarization is the difference of their degrees of polarization and the P.A. direction is the same as that of the dominant mode. With an adequate resulting polarized signal, we can still estimate the RM value. If the modes are not strictly orthogonal, then the net P.A. of the average is the result of a vector summation. This too is of no consequence to RM determination, as long as the relative strength of the two modes and their individual mean P.A. remain constant as a function of radio frequency.

There have been only a few quantitative studies of the frequency dependence of the orthogonal modes (Karastergiou

et al. 2002; Karastergiou & Johnston 2003). In general, the degree of polarization of this pulsar decreases significantly with increasing frequency (Gould & Lyne 1998). In addition, as the observations of Gould & Lyne show, the mode-dominance transition point (longitude of  $\sim 29^\circ$  in Fig. 2) moves to earlier longitudes with increasing radio frequency. This indicates that the relative strengths of the modes *do not* remain constant as a function of frequency. In other words, the first half of the profile, which is predominantly polarized with mode A (*dashed line*) has a steeper spectral index than the second half that is predominantly polarized with mode B (*dot-dashed line*).

In the case of PSR B2016+28, it is also clear that the modes are not exactly orthogonal. The best fit to the two gray scale tracks show that the P.A. and the slope at  $30^\circ$  longitude are  $-42.8 \pm 0.2$  and  $5.04 \pm 0.1 \text{ deg}^{-1}$  for mode A (*dashed line*) and  $49.8 \pm 0.1$  and  $4.37 \pm 0.1 \text{ deg}^{-1}$  for mode B (*dot-dashed line*). These two slope values are significantly different from each other. This P.A. nonorthogonality is known in the literature (Gil et al. 1991, 1992) and has recently been studied in detail by McKinnon (2003). In fact, McKinnon has shown that this is fairly common among several pulsars (e.g., PSRs B0950+08, B1929+10, B2020+28).

#### 5. RM DETERMINATION IN PRESENCE OF QUASI-ORTHOGONAL MODES

Although the fractional polarization seen in the average pulse profiles are typically a few tens of percent, individual pulses can exhibit even higher degree of polarization, some nearly reaching 100% (Stinebring et al. 1984; Rankin,

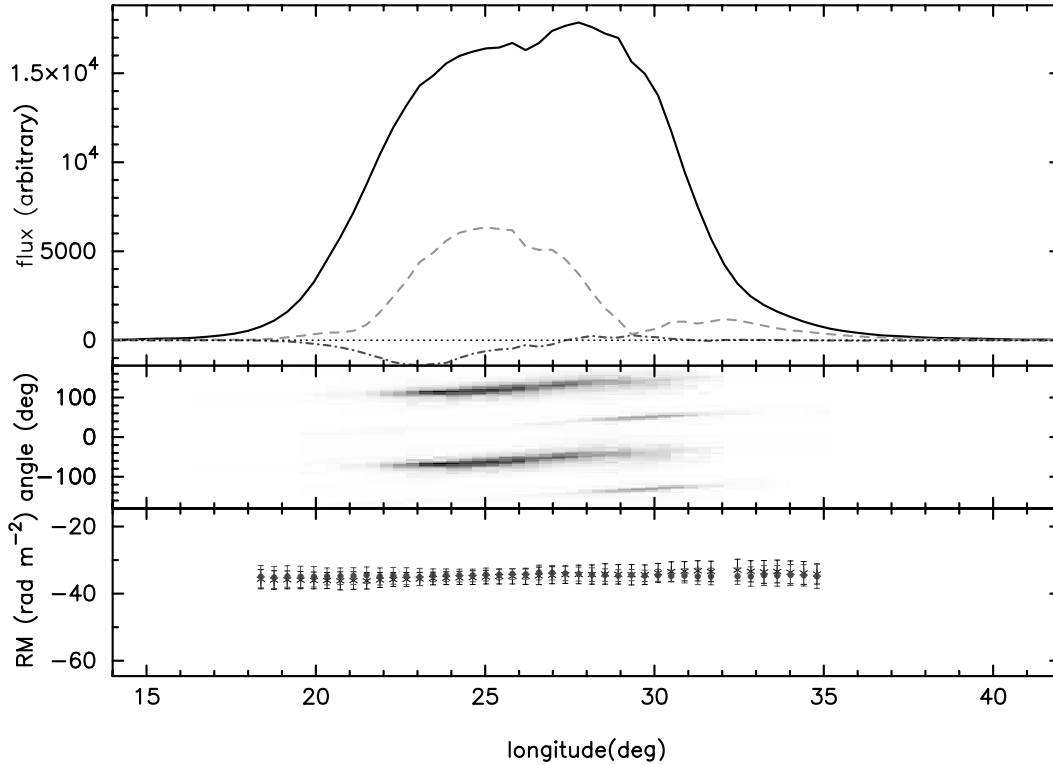


FIG. 3.—Rotation measure of the two polarization modes  $RM_A(\phi)$  and  $RM_B(\phi)$  as a function of pulse longitude. For comparison, we have given average profiles in total power (solid line), linear (dashed line) and circular (dotted line) polarization in the top panel, and the position angle PDF in the middle panel as gray scale. The bottom panel gives the rotation measure of the two modes,  $RM_A(\phi)$  and  $RM_B(\phi)$ . Effective values of RM of the two modes are  $-35.0 \pm 0.4$  and  $-34.5 \pm 0.3$  rad  $m^{-2}$ .

Stinebring, & Weisberg 1989; Ramachandran et al. 2002; Rankin & Ramachandran 2003). Given the presence of the quasi-orthogonal modes and possible depolarization because of their superposition, quite independent of any possible artifacts, it makes sense to determine the RM with individual pulses rather than average pulses.

As described in § 2, our single pulse data set of PSR B2016+28 consists of 3843 pulses, gated to represent a longitude range of about  $45^\circ$  in each pulse. As the first step, in each frequency channel, we produced a P.A. distribution for every longitude. In doing this, we weighted each sample by the square of S/N of the polarized flux. With the assumption that there is no systematic bias of the distribution of P.A.s as a function of the strength of the pulses, this weighting is completely justified. At a given longitude, because of the presence of the two modes, one expects two significant peaks in this distribution separated by almost  $90^\circ$ .

As the second step, we found by a weighted mean the centroid of the two peaks  $[\chi_A(\phi, \nu)$  and  $\chi_B(\phi, \nu)]$ , both being functions of pulse longitude and radio frequency. We thus determined the mean P.A. values of each mode.

Once the P.A.s are determined, then it is straightforward to fit for rotation measure values of the two modes,  $RM_A(\phi)$  and  $RM_B(\phi)$ , as a function of pulse longitude. These two functions determined for PSR B2016+28 are shown in Figure 3. Comparing this to the bottom panel of Figure 2, it is obvious that the deviations of RM values observed for the two modes are far less than what are determined with the average profiles. The effective RM values of the two modes turn out to be  $-35.0 \pm 0.4$  and  $-34.5 \pm 0.3$  rad  $m^{-2}$ , respectively. These values are very close to the earlier measurement of  $-34.6 \pm 1.4$  rad  $m^{-2}$  (Manchester 1972).

As emphasized in § 4, the presence of the two modes itself, even if they are not orthogonal, should not introduce any artifact in RM measurements, as long as there is no frequency dependence of the relative strength and the intrinsic P.A.s of the two modes. However, in our analysis of PSR B2016+28, the value of  $RM(\phi)$  is significantly different from the values of  $RM_A(\phi)$  and  $RM_B(\phi)$ , which clearly indicates that the incoherent superposition of the modes while generating average profiles (as a function of frequency) has introduced a frequency dependence of the resulting P.A., which manifests as *extra* RM.

To investigate this subtle effect in detail, with the help of the procedure described above, we produced Figure 4, which shows the nonorthogonality of the two modes as a function of pulse longitude. We have plotted the quantity

$$\Delta\psi(\phi) = \frac{\pi}{2} - \langle [\chi_B(\phi, \nu) - \chi_A(\phi, \nu)] \rangle_\nu \quad (3)$$

against pulse longitude  $\phi$ . The deviations are not uniform across the pulse profile, and the variations are statistically significant.

Let  $X_A(t, \nu)$  and  $X_B(t, \nu)$  be the “instantaneously” randomly varying linearly polarized intensities of the two quasi-orthogonal modes. Let  $\zeta(\nu)$  be the angle between the two vectors in the Stokes  $Q$ - $U$  space. Assuming that the P.A. of the primary mode is zero, we can write the two Stokes parameters  $Q$  and  $U$  as (see also McKinnon 2003)

$$\begin{aligned} Q(t, \nu) &= X_A(t, \nu) + X_B(t, \nu) \cos \zeta(\nu) + X_Q(t, \nu), \\ U(t, \nu) &= X_B(t, \nu) \sin \zeta(\nu) + X_U(t, \nu). \end{aligned} \quad (4)$$

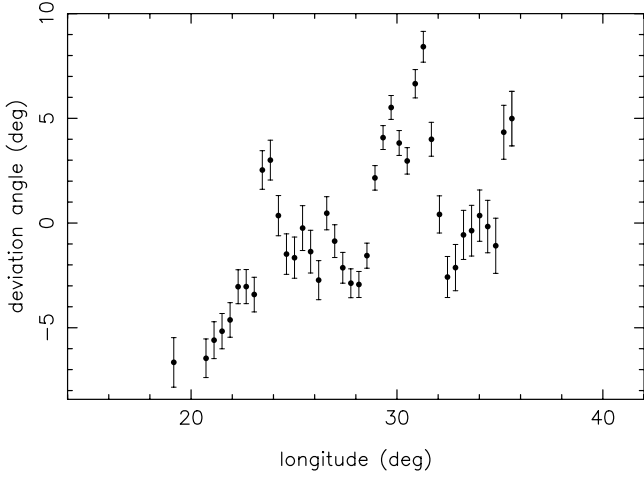


FIG. 4.—Average deviation angle ( $y$ -axis) from nonorthogonality of the two polarization modes as a function of pulse longitude ( $x$ -axis). See text for details.

If  $\zeta(\nu)$  is independent of  $X_A(t, \nu)$ , then P.A. as a function of frequency with average values of  $Q$  and  $U$  is

$$\begin{aligned} \langle \chi_{AB}(\nu) \rangle &= \frac{1}{2} \tan^{-1} \left[ \frac{\langle U(t, \nu) \rangle}{\langle Q(t, \nu) \rangle} \right] \\ &= \frac{1}{2} \tan^{-1} \left[ \frac{\sin \zeta(\nu)}{F_{AB}(\nu) + \cos \zeta(\nu)} \right] \end{aligned} \quad (5)$$

where the angular brackets indicate time-averaging and  $F_{AB}(\nu) = \langle X_A(t, \nu) \rangle / \langle X_B(t, \nu) \rangle$ . The variables  $X_Q(t, \nu)$  and  $X_U(t, \nu)$  are the system noise strengths in  $Q$  and  $U$  as a function of time and frequency. As we can see, in principle, frequency dependence in  $\zeta(\nu)$  or  $F_{AB}(\nu)$  can introduce a frequency dependent  $\langle \chi_{AB}(\nu) \rangle$ , which can corrupt our rotation measure determination.

The dependence of  $\langle \chi_{AB}(\nu) \rangle$  on frequency is different from that of the RM. Therefore, in principle, the RM measured at different frequency ranges should be different. To check this, we divided our frequency band into two parts. Indeed, the value of  $\text{RM}(\phi)$  was different in the two halves. In the first half of the band, the measured value of RM was  $-32.5 \pm 0.9 \text{ rad m}^{-2}$ , whereas in the other, it was  $-40.5 \pm 0.4 \text{ rad m}^{-2}$ . The overall value of  $\langle \text{RM} \rangle$  was  $-38.3 \pm 0.6 \text{ rad m}^{-2}$ .

The error introduced by this effect depends on the bandwidth, the center frequency, and the frequency dependences of  $\zeta(\nu)$  and  $F_{AB}(\nu)$ . Figure 5 succinctly summarizes this effect. This theoretically generated plot corresponds to a center frequency of 430 MHz and a bandwidth of 10 MHz, which is divided into 128 frequency channels. In the left panel, we place  $\zeta(\nu)$  on the  $x$ -axis and the effective RM introduced by this quasi-orthogonal mode-mixing on the  $y$ -axis. The five curves, solid, dashed, dot-dashed, dotted, and triple-dot-dashed, correspond to variations of fractional strength of the two modes  $[F_{AB}(\nu)]$  from the lower to the upper end of the frequency band of 0.3–0.9, 0.45–0.9, 0.6–0.9, 0.75–0.9, and a constant 0.9, respectively. When the relative strength remains constant, then the RM introduced by this effect is zero. However, when the relative strength varies as a function of frequency, then the spurious RM introduced in the measurement could be significant.

In the right panel of Figure 5, we have addressed the other possibility that for a constant fractional strength across the frequency band,  $\zeta(\nu)$ , varies. The five curves, solid, dashed,

dot-dashed, dotted, and triple-dot-dashed, correspond to  $\zeta(\nu)$  varying in the ranges of  $160^\circ$ – $180^\circ$ ,  $165^\circ$ – $180^\circ$ ,  $170^\circ$ – $180^\circ$ ,  $175^\circ$ – $180^\circ$ , and a constant value of  $180^\circ$ , respectively. Here, the RM value changes sign at  $F_{AB}(\nu) = 1$ , and this is exactly what we see in Figure 2. The inferred value of  $\text{RM}(\phi)$  has an antisymmetry with respect to  $\phi \sim 30^\circ$ , where one mode is stronger to the right and the other mode to the left. It is worth noting here that in Figure 5, at the limit of  $F_{AB}(\nu) \rightarrow \infty$ , the RM introduced asymptotically reduces to zero.

## 6. DISCUSSION

In Figures 1 and 2, that the value  $\text{RM}(\phi)$  does not remain constant between various epochs of observation is intriguing. Perhaps one reason could be a combination of interstellar scintillation and the effect that we have addressed in this paper. Although scintillation is not expected to have any effect on the amount of Faraday rotation introduced in the interstellar medium, when the total integration time is short ( $\sim$ a few minutes), the effective center frequency and bandwidth are expected to vary. Combined with the effect that we have described, the RM value inferred in principle can be different at different epochs. Moreover, as described in § 2, each panel in Figure 1 has been produced with 120 s ( $\sim$ 200 pulses) long scans. Pulsars are known to exhibit stable average-pulse profiles only after integrating a few thousand pulses. As we can see from the four panels, average profiles, and even polarization-sweep curves, are not identical between all the panels. This may also introduce time dependence in RM values.

As mentioned in § 5, the exact frequency dependence of  $F_{AB}(\nu)$  and  $\zeta(\nu)$  are not known. In general, there is no reason to conclude that the frequency dependence of  $\langle \chi_{AB}(\nu) \rangle$  introduced by this effect is the same as that of the RM. We have attempted in Figure 5 to estimate the effective RM introduced by this effect. A thorough investigation of the nature of the emission modes and their frequency dependence is beyond the scope of this paper, and we plan to consider these matters in a subsequent report.

As radiation from pulsars is highly polarized and as distance estimates to pulsars are more reliable than to other polarized sources (e.g., supernova remnants), pulsar RM determinations have been used extensively in probing the magnetic field structure of the Galaxy. RM is an important tool for modeling the long-range as well as the turbulent component of the Galactic magnetic field. If the effect that we have discussed in this paper is common, then it will have serious consequences on the existing RM measurements of pulsars and therefore on the models of magnetic field structure in the Galaxy. Apart from our detailed analysis of PSR B2016+28 presented here, in the sample of Weisberg et al. (2004), we looked at pulsars B0301+19, B0525+21, B0626+24, B1929+10, and B2020+28. These all showed systematic variation of the RM across the pulse profile. For instance, Weisberg et al. measure RM values for these pulsars of  $-5.7 (\pm 10)$ ,  $-39.2 (\pm 10)$ ,  $69.5 (\pm 10)$ ,  $-5.9 (\pm 5)$ , and  $-73.7 (\pm 25) \text{ rad m}^{-2}$ , respectively. The values given in parenthesis are the approximate magnitude of variations seen around the mean value across the pulse profile. As we can clearly see, these variations are significant. Especially when the magnitude of RM is small, these variations can cause significant bias.

The presence of orthogonal modes is common among pulsars. Among pulsars for which any detailed single-pulse studies have been done so far, it is clear that a great majority of them exhibit orthogonal modes. In particular, it is almost impossible to find a “conal” pulsar that does not show

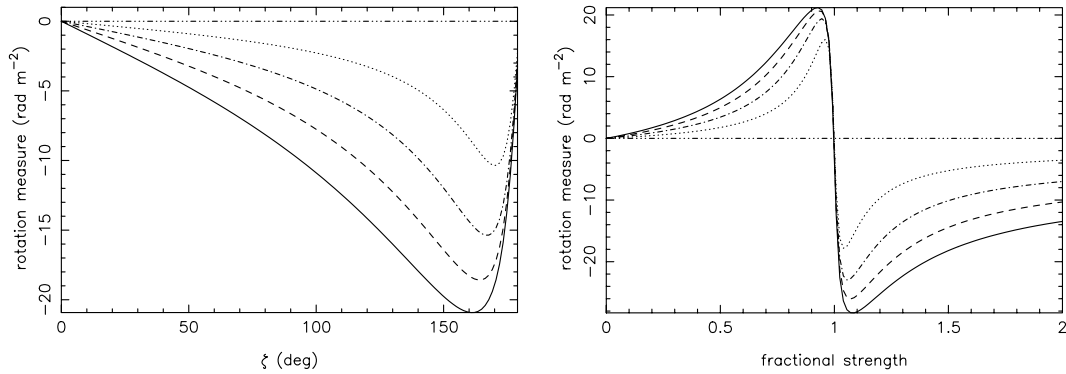


FIG. 5.—Effective RM introduced by nonorthogonal mode-mixing ( $y$ -axis). The left panel shows RM as a function of  $\zeta(\nu)$ . For a constant  $\zeta(\nu)$  value, the five curves, solid, dashed, dot-dashed, dotted and triple-dot-dashed, correspond to variations of fractional strengths of the two modes  $[F_{AB}(\nu)]$  from the lower to the upper end of the frequency bands of 0.3–0.9, 0.45–0.9, 0.6–0.9, 0.75–0.9, and a constant 0.9, respectively. In the right panel, the five curves correspond to variation of  $\zeta(\nu)$  of  $160^\circ$ – $180^\circ$ ,  $165^\circ$ – $180^\circ$ ,  $170^\circ$ – $180^\circ$ ,  $175^\circ$ – $180^\circ$ , and a constant value of  $180^\circ$ , respectively. See text for details.

evidence of orthogonal mode emission associated with its conal components (Rankin & Ramachandran 2003). It is also possible that these two modes have significantly different spectral indices. For instance, there is clear evidence to show that the degree of polarization in the average-pulse profiles decreases with increasing frequency. This can be understood easily by having one of the modes dominating in strength at lower frequencies, and the two modes having roughly comparable strengths at very high frequencies. As earlier studies (Stinebring et al. 1984; Gil et al. 1991, 1992; McKinnon 2003) have shown, these modes are slightly nonorthogonal, and this non-orthogonality of the two modes is a widespread phenomenon.

As we have shown in this paper, the only way to eliminate this artifact is to determine RM values from single pulses. This, of course, is a very challenging task, owing to signal-to-noise ratio considerations. For weaker pulsars for which we cannot obtain good single-pulse data, it is impossible to separate the two modes to unambiguously determine RM values. Therefore, weaker pulsars are bound to suffer from this artifact, and there is no obvious way of correcting it.

On the Galactic scale, whether or not this effect will make serious changes to the magnetic field model remains to be seen. A project to determine correct RM values for several other pulsars is underway and will be presented in a subsequent publication. It is conceivable that this artifact will be most prominent among pulsars with small RM magnitudes ( $\leq 50 \text{ rad m}^{-2}$  or so). A thorough analysis to check the validity of the already existing RM values and the effect on the Galactic magnetic field structure is much needed.

## 7. CONCLUSION

Our major conclusions from this work can be summarized as follows:

1. We find that the rotation measures determined for PSR B2016+28 as a function of pulse longitude vary significantly. This seems to be the case for five other pulsars, namely, PSRs B0301+19, B0525+21, B0626+24, B1929+10, and B2020+28.
2. This effect is an artifact introduced by the frequency dependence of relative strengths of the two modes, as well as the amount of nonorthogonality, and it is not intrinsic to the pulsar magnetosphere. We show that if we estimate rotation measure for the two modes separately, this effect can be removed. The technique to remove this artifact invariably involves analysis with single pulses and hence cannot be carried out for fainter objects. There is no other obvious way of compensating for this artifact for these fainter objects.
3. As the amount of RM spuriously introduced can be as high as a few tens of units, several measurements of rotation measures of pulsars in the literature may be in error and need revision.

We thank Jon Arons, Avinash Deshpande, Aris Karastergiou, Simon Johnston, Michael Kramer & Dipanjan Mitra for useful comments on the manuscript. Special thanks are due to Dipanjan Mitra, Simon Johnston and Michael Kramer for sharing their result of RM changes as a function of pulse longitude prior to publication. We also thank our anonymous referee for his/her valuable comments.

## REFERENCES

- Backer, D. C., & Rankin, J. M. 1980, *ApJS*, 42, 143  
 Gil, J. A., Lyne, A. G., Rankin, J. M., Snakowski, J. K., & Stinebring, D. R. 1992, *A&A*, 255, 181  
 Gil, J. A., Snakowski, J. K., & Stinebring, D. R. 1991, *A&A*, 242, 119  
 Gould, D. M., & Lyne, A. G. 1998, *MNRAS*, 301, 235  
 Guojun, Q., Manchester, R. N., Lyne, A. G., & Gould, D. M. 1995, *MNRAS*, 274, 572  
 Hamilton, P. A., & Lyne, A. G. 1987, *MNRAS*, 224, 1073  
 Hamilton, P. A., McCulloch, P. M., Manchester, R. N., Ables, J. G., & Komersaroff, M. M. 1977, *Nature*, 265, 224  
 Han, J. L., Manchester, R. N., & Qiao, G. J. 1999, *MNRAS*, 306, 371  
 Indrani, C., & Deshpande, A. A. 1998, *NewA*, 4, 33  
 Karastergiou, A., & Johnston, S. 2003, *A&A*, 404, 325  
 Karastergiou, A., Kramer, M., Johnston, S., Lyne, A. G., Bhat, N. D. R., & Gupta, Y. 2002, *A&A*, 391, 247  
 Manchester, R. N. 1972, *ApJ*, 172, 43  
 ———. 1974, *ApJ*, 188, 637  
 McKinnon, M. 2003, *ApJ*, 590, 1026  
 Melrose, D. C. 1979, *Australian J. Phys.*, 32, 61  
 Mitra, D., Wielabinski, R., Kramer, M., & Jessner, A. 2003, *A&A*, 398, 993  
 Petrova, S. A. 2001, *A&A*, 378, 883  
 Petrova, S. A., & Lyubarskii, Y. E. 2000, *A&A*, 355, 1168  
 Radhakrishnan, V., & Cooke, D. J. 1969, *Astrophys. Lett.*, 3, 225  
 Radhakrishnan, V., & Deshpande, A. A. 2001, *A&A*, 379, 551  
 Ramachandran, R., Rankin, J. M., Stappers, B. W., Kouwenhoven, M. L. A., & van Leeuwen, A. G. J. 2002, *A&A*, 381, 993  
 Rand, R. J., & Lyne, A. G. 1994, *MNRAS*, 268, 497  
 Rankin, J. M., Campbell, D. B., Isaacman, R. B., & Payne, R. R. 1988, *A&A*, 202, 166  
 Rankin, J. M., & Ramachandran, R. 2003, *ApJ*, 590, 411  
 Rankin, J. M., & Rathnasree, N. 1995, *J. Astrophys. Astron.*, 16, 327  
 Rankin, J. M., Stinebring, D. R., & Weisberg, J. M. 1989, *ApJ*, 346, 869  
 Stinebring, D. R., Cordes, J. M., Weisberg, J. M., Rankin, J. M., & Boriakoff, V. 1984, *ApJS*, 55, 247  
 Thompson, R. C., & Nelson, A. H. 1980, *MNRAS*, 191, 863  
 Weisberg, J. M., et al., 2004, *ApJS*, 150, 317